

Hierlinger C, Flint HV, Cordes DB, Slawin AMZ, Gibson EA, Jacquemin D,  
Guerchais V, ZysmanColman E.

[A Panchromatic, Near Infrared Ir\(III\) Emitter Bearing a Tripodal C<sup>N</sup>C ligand  
as a Dye for Dye-Sensitized Solar Cells.](#)

*Polyhedron* 2017,

<https://doi.org/10.1016/j.poly.2017.12.003>

**Copyright:**

© 2017. This manuscript version is made available under the [CC-BY-NC-ND 4.0 license](#)

**DOI link to article:**

<https://doi.org/10.1016/j.poly.2017.12.003>

**Date deposited:**

19/12/2017

**Embargo release date:**

09 December 2018



This work is licensed under a  
[Creative Commons Attribution-NonCommercial-NoDerivatives 4.0 International licence](#)

# A Panchromatic, Near Infrared Ir(III) Emitter Bearing a Tripodal C<sup>N</sup>C ligand as a Dye for Dye-Sensitized Solar Cells

Claus Hierlinger,<sup>a,b</sup> Heather V. Flint,<sup>c</sup> David B. Cordes,<sup>b</sup> Alexandra M. Z. Slawin,<sup>b</sup> Elizabeth A.

Gibson<sup>\*c</sup> Denis Jacquemin,<sup>\*d</sup> Véronique Guerschais,<sup>\*a</sup> Eli Zysman-Colman<sup>\*b</sup>

<sup>a</sup> Institut des Sciences Chimiques de Rennes, UMR 6226 CNRS-Université de Rennes 1, Campus de Beaulieu, 35042 Rennes Cedex, France. E-mail: veronique.guerchais@univ-rennes1.fr

<sup>b</sup> Organic Semiconductor Centre, EaStCHEM School of Chemistry, University of St Andrews, St Andrews, Fife, KY16 9ST, UK. E-mail: eli.zysman-colman@st-andrews.ac.uk; Web:

<http://www.zysman-colman.com>

<sup>c</sup> Chemistry, School of Natural and Environmental Science, Newcastle University, Newcastle upon Tyne, NE1 7RU, UK. Elizabeth.gibson@ncl.ac.uk

<sup>d</sup> UMR CNRS 6230, Université de Nantes, CEISAM, 2 rue de la Houssinière, 44322 Nantes Cedex 3, France. E-mail: Denis.Jacquemin@univ-nantes.fr

## Abstract

The synthesis of a new complex of the form [Ir(C<sup>N</sup>C)(N<sup>N</sup>)Cl] [where C<sup>N</sup>C = 2-(bis(4-(*tert*-butyl)phenyl)methyl)pyridinato (dtBubnpy, **L1**) and N<sup>N</sup> is diethyl [2,2'-bipyridine]-4,4'-dicarboxylate (deeb)] is reported. The crystal structure reveals an unusual tripodal tridentate C<sup>N</sup>C ligand forming three six-membered rings around the iridium center. The photophysical and electrochemical properties suggest the use of this complex as a dye in dye-sensitized solar

cells. Time-Dependent Density Functional Theory (TD-DFT) calculations have been used to reveal the nature of the excited-states.

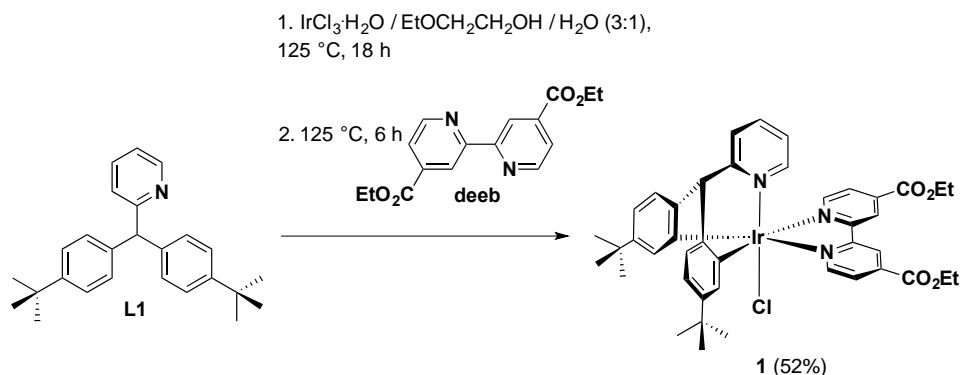
## Introduction

Dye-sensitized solar cells (DSSCs) represent a promising solar cell technology. The majority of champion DSSCs, those showing power conversion efficiencies (PCE) greater than 10%, are based on ruthenium(II) complexes. Iridium(III) complexes, dominant as emitters in electroluminescent devices,[1,2] have to date fared poorly as dyes in DSSCs.[3-13] This is mainly because most iridium(III) complexes are not panchromatic, having absorption spectra that tail off by 550 nm. This induces low short circuit currents in the DSSC and as a consequence poor PCE; typically less than 4%. Indeed, there are very few examples of iridium(III) complexes with significant absorption bands going up to the red or NIR parts of the visible spectrum.[14-20,12]

We recently reported the development of tripodal C<sup>N</sup>C ligands, 2-benzhydrylpyridine and its derivatives, which can coordinate to iridium, forming three six-membered chelate rings through a double C-H bond activation.[21] When combined with a bidentate diimine ligand such as 4,4'-diterbutyl-2,2'-bipyridine (dtBubpy), a family of orange-to-red emitting neutral [Ir(C<sup>N</sup>C)(dtBubpy)Cl] complexes was formed with absorption bands tailing off at 600 nm. Herein, we report an analogous complex showing panchromatic absorption, employing an electron-poor ancillary ligand diethyl [2,2'-bipyridine]-4,4'-dicarboxylate (deeb), and study its use as a DSSC dye.

## Results and Discussion

## Synthesis



Scheme 1: Scheme for the one-pot synthesis of complex **1**.

Compound **L1**[21] and deeb[22] were prepared by literature methods. Complex **1** was obtained as a black solid in 52% yield using a two-step-one-pot protocol wherein a mixture of **L1** and  $\text{IrCl}_3 \cdot 6\text{H}_2\text{O}$  in 2-ethoxyethanol/ $\text{H}_2\text{O}$  (3:1) was heated at reflux for 19 h followed by the addition of deeb and a further reaction time of 6 h (Scheme 1). Complex **1** was characterized by  $^1\text{H}$  and  $^{13}\text{C}$  NMR spectroscopy, HR-ESI mass spectrometry, elemental analysis and melting point determination [see Figures S1-6 in the Supporting Information (SI) for NMR and HR-ESI mass spectra].

## Crystal Structures

Single crystals of sufficient quality of **1** were grown from  $\text{CH}_2\text{Cl}_2/\text{Et}_2\text{O}$  at  $-18^\circ\text{C}$ , and the structure of **1** was determined by single-crystal X-ray diffraction (Figure 1, Table S1). Complex **1**,  $[\text{Ir}(\text{L1})(\text{deeb})\text{Cl}]$ , lies in a mirror plane; the pyridyl ring of **L1**, the iridium(III) and the chloride all lying directly in the plane. The tridentate **L1** shows a tripodal chelation motif, analogous to that seen previously.[21] The remaining coordination sphere of **1** consists of the deeb  $\text{N}^{\wedge}\text{N}$  ligand and a chloride anion. The arrangement of ligands is unusual, as the chloride coordinates *trans* to the

pyridine of **L1** and not *trans* to a cyclometalated carbon ligand as generally observed in tridentate complexes,[23-27] although this coordination arrangement was found in our previous complexes based on **L1**. [21] The Ir-Cl bond is 2.346(3) Å, which is within the range of distances we have previously reported for [Ir(C<sup>^</sup>N<sup>^</sup>C)(dtBubpy)Cl] complexes (where C<sup>^</sup>N<sup>^</sup>C is a substituted 2-benzhydrylpyridine),[21] and is similar to the Ir-Cl distance seen in the related complex [Ir(tpy)(dmbpy)Cl]<sup>2+</sup> (where tpy = 2,2':6',2''-terpyridine and dmbpy = 4,4'-dimethyl-2,2'-bipyridine).[28] The Ir-N<sub>N<sup>^</sup>N</sub> bonds [2.134(6) Å] are in the same range as both our related [Ir(C<sup>^</sup>N<sup>^</sup>C)(dtBubpy)Cl] complexes,[21] as well as the deeb complex [Ir(topy)<sub>2</sub>(deeb)]PF<sub>6</sub> [where topyH = 2-(*p*-tolyl)pyridine].[29] The Ir-N distance involving the nitrogen from **L1** [2.038(8) Å] is markedly shorter than the Ir-N<sub>N<sup>^</sup>N</sub> distance. The Ir-C<sub>C<sup>^</sup>N<sup>^</sup>C</sub> bonds [2.027(7) Å] are shorter again than the Ir-N bonds, in agreement with our previous observations.[21] The bite angle of the N<sup>^</sup>N ligand is 76.1(3)°, in line with other iridium complexes possessing bidentate diimine ancillary ligands.[30-33,21] The C-Ir-C angle [85.2(4)°] and N-Ir-C angle within **L1** [88.0(2)°] are significantly larger due to the formation of three 6 membered chelate rings in the C<sup>^</sup>N<sup>^</sup>C ligand.

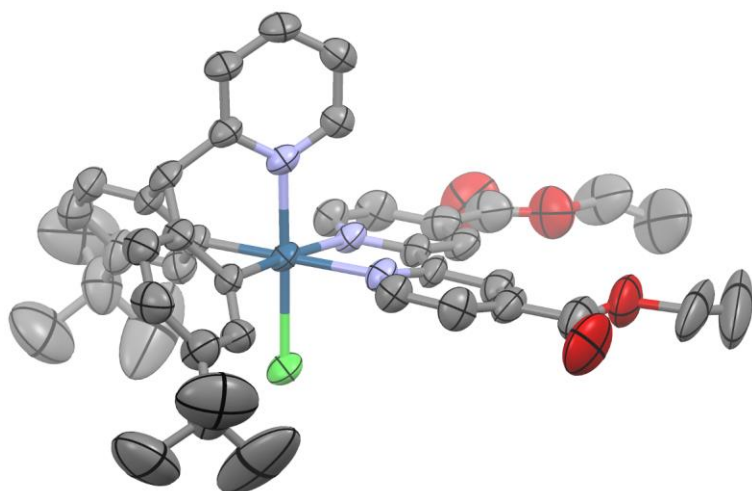


Figure 1. Solid-state structure of complex **1**, thermal ellipsoids are drawn at the 50 % probability level. Hydrogen atoms and solvent molecules are omitted for clarity (color code: C = grey, N = purple, O = red, Cl = green and Ir = blue).

### *Electrochemical properties*

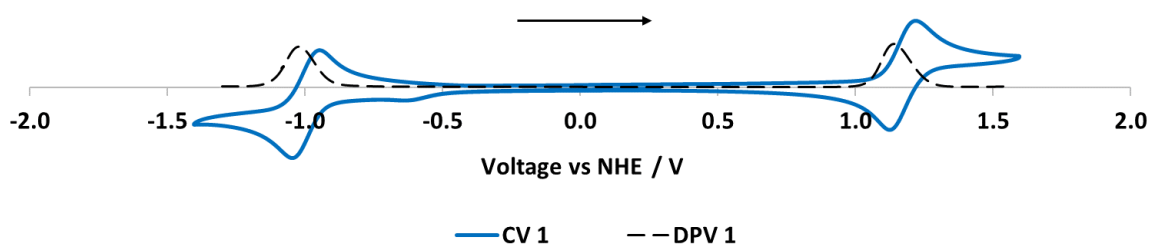


Figure 2. Cyclic voltammograms (in blue solid lines) and differential pulse voltammetry (in dotted black lines) carried out in degassed  $\text{CH}_2\text{Cl}_2$  at a scan rate of  $100 \text{ mV s}^{-1}$ , with  $\text{Fc}/\text{Fc}^+$  as the internal reference, referenced to NHE ( $0.70 \text{ V vs. NHE}$ ).[34]

The electrochemical properties of **1** were evaluated by cyclic voltammetry (CV) and differential pulse voltammetry (DPV) in deaerated  $\text{CH}_2\text{Cl}_2$  solution at  $298 \text{ K}$  at a scan rate of  $100 \text{ mV s}^{-1}$  using  $\text{Fc}/\text{Fc}^+$  as the internal reference and referenced with respect to NHE ( $0.70 \text{ V vs. NHE}$ ).[34] The electrochemical data are summarized in Table 1 and the voltammograms are shown in Figure 2. Complex **1** exhibits a quasi-reversible single electron oxidation wave at  $1.21 \text{ V}$ , which is assigned to the  $\text{Ir(III)}/\text{Ir(IV)}$  redox couple, with contributions from the two phenyl rings of **L1** and the chloro ligand. Compared to  $[\text{Ir}(\text{L1})(\text{dtBubpy})\text{Cl}]$ , **R1**, (Figure 3,  $E_{1/2}^{\text{ox.}} 1.04 \text{ V vs. NHE}$ )[21] the oxidation potential in **1** is significantly anodically shifted by  $170 \text{ mV}$ , reflecting the electron-withdrawing capacity of the ethyl ester groups of the  $\text{N}^{\wedge}\text{N}$  ligand, which modifies the

electron density on iridium. However, the oxidation potential of **1** is less positive than that of [Ir(ppy)<sub>2</sub>(deeb)]PF<sub>6</sub>, **R2**, ( $E_{1/2}^{ox} = 1.57$  V in deaerated MeCN vs NHE, where ppy is 2-phenylpyridinato).[35] Upon scanning to negative potential, **1** shows a single quasi-reversible reduction wave at -0.94 V, which is monoelectronic as inferred from the DPV. The electron-withdrawing effect of the ethyl ester groups of the N<sup>^</sup>N ligand results in a large anodic shift of 610 mV in the reduction wave of **1** compared to **R1** ( $E_{1/2}^{red} = -1.58$  V vs NHE).[21] Complex **R2** showed two reversible reduction waves in MeCN. The first reduction located at -0.76 V is assigned to the reduction of the deeb ligand while the second one at -1.30 V is due to the reduction of the phenylpyridinato.[35] Thus, the reduction of the deeb ligand in **1** is shifted to more negative potentials compared to the same reduction in **R2**. DFT calculations of the previously reported **R1** indicated that both the HOMO and HOMO-1 are close in energy and involve the iridium and chlorine atoms and the two phenyl rings of **L1**. [21] As can be seen in Figure 4 the same electron density distribution is found in **1**. DFT calculations also show that the three lowest unoccupied orbitals are exclusively localized on the deeb ligand in **1** (Figure 4), while the LUMO+1 is primarily on the pyridyl of **L1** in **R1**, illustrating the stronger accepting character of deeb. The  $\Delta E_{redox}$  for **1** (2.18 eV) is markedly smaller than that of **R2** ( $\Delta E_{redox} = 2.33$  V).[35]

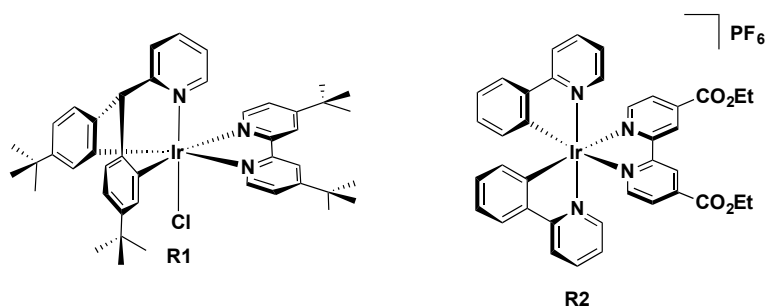


Figure 3. Structures of reference complexes **R1** and **R2**.

Table 1: Selected electrochemical properties of complex **1**

Electrochemistry <sup>a</sup>							
	$E_{1/2}^{ox} / \text{V}$	$\Delta E_p / \text{mV}$	$E_{1/2}^{red} / \text{V}$	$\Delta E_p / \text{mV}$	$\Delta E_{redox}^b / \text{V}$	$E_{HOMO}^c / \text{eV}$	$E_{LUMO}^c / \text{eV}$
<b>1</b>	1.21	88	-0.97	99	2.18	-5.31	-3.13

<sup>a</sup> in degassed CH<sub>2</sub>Cl<sub>2</sub> at a scan rate of 100 mV s<sup>-1</sup> with Fc/Fc<sup>+</sup> as internal reference, and referenced with respect to NHE (Fc/Fc<sup>+</sup> = 0.70 V in CH<sub>2</sub>Cl<sub>2</sub>); [36,34,37] <sup>b</sup> $\Delta E_{redox}$  is the difference (V) between first oxidation and first reduction potentials; <sup>c</sup>  $E_{HOMO/LUMO} = -[E^{ox/red} \text{ vs Fc/Fc}^+ + 4.8]$  eV.[34]

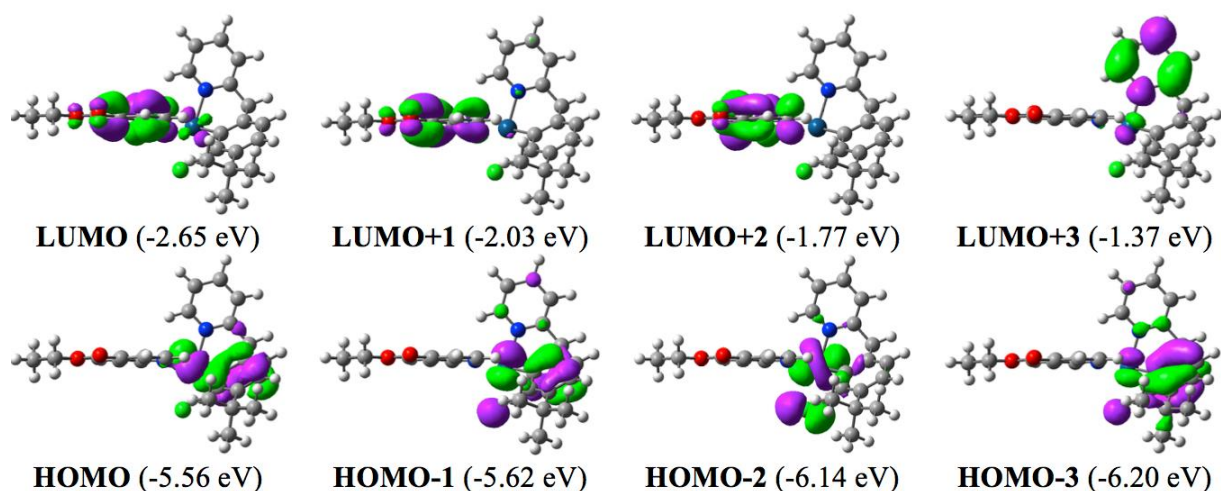


Figure 4. Frontier molecular orbitals of **1** computed through DFT (M06 functional, see the SI for details) and represented using a contour threshold of 0.03 au.

### Photophysical properties

The photophysical data for **1** recorded in CH<sub>2</sub>Cl<sub>2</sub> at 298 K are shown in Figure 5 and the data summarized in Table 2. The absorption profile of **1** differs significantly from that of **R1**. Complex **1** shows intense high-energy absorption bands ( $\epsilon$  on the order of  $3.5 \times 10^4 \text{ M}^{-1} \text{ cm}^{-1}$ ) below 250 nm, which are ascribed to  $^1\pi-\pi^*$  ligand-centered ( $^1\text{LC}$ ) transitions localized on the deeb ligand. A moderately intense band ( $\epsilon$  on the order of  $1.5 \times 10^4 \text{ M}^{-1} \text{ cm}^{-1}$ ) at 319 nm is assigned to



a ligand-centered (LC) transition on the deeb with a small CT character (see below). Weaker bands ( $\epsilon$  on the order of  $5\text{-}6 \times 10^3$  and  $2 \times 10^3 \text{ M}^{-1} \text{ cm}^{-1}$ ) in the region of 380 – 440 nm and tailing to 500 - 600 nm are attributed to a mixture of ( $^1\text{MLCT}/^1\text{LLCT}$ ) and spin-forbidden ( $^3\text{MLCT}/^3\text{LLCT}$ ) transitions involving the deeb ligand. Iridium(III) complexes often do not show absorption onsets lower in energy than 550 nm;[38-40] though, there are known examples of neutral Ir(III) complexes showing absorption bands beyond 550 nm.[41,25,42,43]

The assignments for complex **1** were confirmed by TD-DFT calculations (see the ESI for technical details). The two lowest singlet states, computed at 623 and 611 nm, present relatively small intensities (oscillator strengths,  $f$ , of 0.010 and 0.056, respectively) and mainly correspond to HOMO-1 to LUMO and HOMO to LUMO transitions. As can be seen in Figure 4, this clearly corresponds to a mixed CT process from the metal and the phenyl rings of the C<sup>N</sup>C ligand towards the deeb. The following significant vertical absorption are predicted by TD-DFT at 496 nm ( $f=0.071$ ), 456 nm ( $f=0.027$ ) and 443 nm ( $f=0.084$ ) and these bands can be ascribed to HOMO-2 to LUMO, HOMO to LUMO+1 and HOMO-1 to LUMO+1 transitions, respectively, and therefore all involve strong CT character towards the deeb moiety. The more intense and resolved band at 319 nm experimentally (see Table 2) is computed at 315 nm by TD-DFT ( $f=0.162$ ) and corresponds to a more LC excitation from a low-lying orbital centered on the deeb (and partly on chlorine atom) towards the LUMO centered on the deeb as well.

Upon photoexcitation at 420 nm, **1** exhibits a broad featureless profile, indicative of an emission with mixed CT character, with a maximum at  $\lambda_{\text{em}} = 731 \text{ nm}$ , an emission that is significantly redshifted (99 nm,  $2194 \text{ cm}^{-1}$ ) compared to **R1** ( $\lambda_{\text{em}} = 630 \text{ nm}$ ).[21] The red-shifted

luminescence is due to the presence of the presence of the  $\pi$ -accepting deeb. The emission of **1** is likewise red-shifted (51 nm, 2194 cm<sup>-1</sup>) compared to that of **R2** ( $\lambda_{em}$  = 680 nm).[35] The DFT calculations returns an emission of the T<sub>1</sub> state at 762 nm, close to the experimental value, confirming emission from the lowest triplet excited state. The topology of this state, in terms of localization of the excess  $\alpha$  electrons, is displayed in Figure 6. As can be seen, the spin density is mostly localized on the Ir and Cl atoms and on the ancillary ligand, the tridentate ligand playing only a minor role in this state. This localization is consistent with the observed red-shift in emission compared to **R1** and **R2**. The measured photoluminescence quantum yield ( $\Phi_{PL}$ ) of **1** is 0.5%, lower than those of **R1** (6%) and **R2** (5%), a logical consequence of the energy gap law. Among near-infrared emissive cationic Ir(III) emitters with  $\lambda_{em}$  beyond 700 nm bearing diimines as ancillary ligand, most examples exhibit  $\Phi_{PL}$  values less than 4%.[40,44-47] However, NIR-emitting neutral Ir(III) complexes of the form [Ir(C<sup>^</sup>N)<sub>2</sub>(O<sup>^</sup>O)] (where O<sup>^</sup>O a substituted  $\beta$ -diketonate ancillary ligand) employing highly conjugated C<sup>^</sup>N ligands have reached  $\Phi_{PL}$  of up to 16%.[48,41,49] Complex **1** exhibits a multiexponential emission decay, a reflection of the large non-radiative decay rate constant.

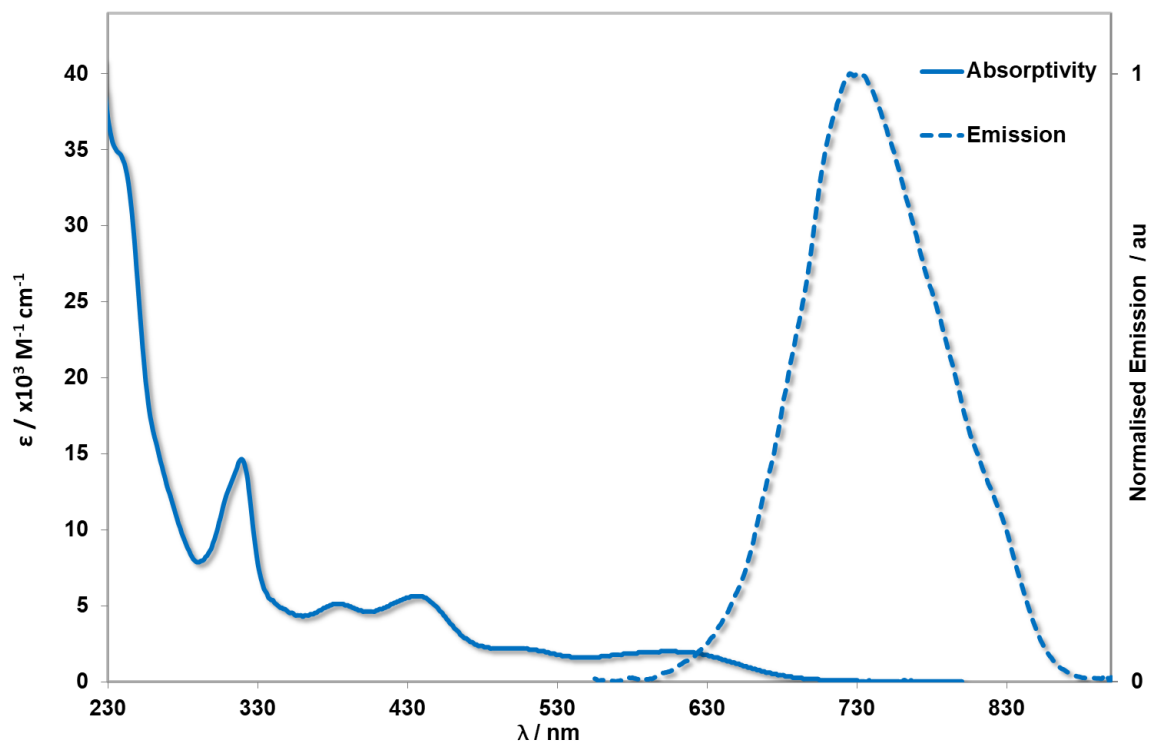


Figure 5. The absorptivity (solid line) and photoluminescence spectra (dotted line) of **1** in CH<sub>2</sub>Cl<sub>2</sub> at 298 K.

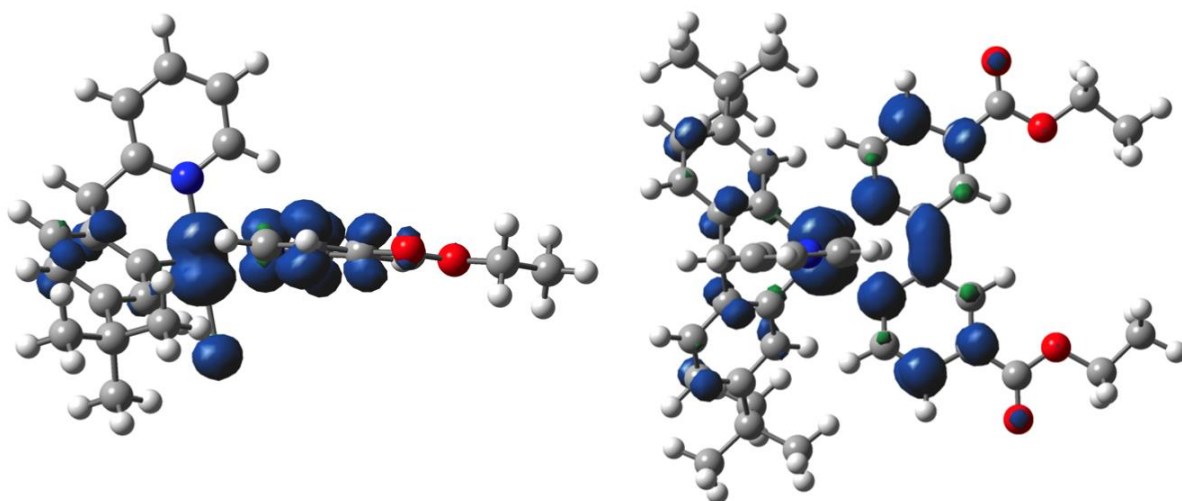


Figure 6. DFT computed spin density difference plots for the lowest triplet state of **1**. Both side and top views are shown and they have been drawn with a contour threshold of  $3 \times 10^{-3}$  au.

Table 2. Photophysical properties of complex **1**.

Complex	$\lambda_{\text{abs}} / \text{nm}$ ( $\epsilon / \text{M}^{-1}\text{cm}^{-1}$ ) <sup>a</sup>	$\lambda_{\text{em}}^{\text{b}} / \text{nm}$	$\Phi_{\text{PL}}^{\text{b,c}} / \%$	$\tau_{\text{e}}^{\text{d}} / \text{ns}$
<b>1</b>	237 (34819), 319 (14647), 384 (5105),	731	0.5	36 (73 %)
	434 (5607), 504 (2176), 597 (1925)			78 (19 %)
				392 (8 %)

<sup>a</sup> Recorded in aerated  $\text{CH}_2\text{Cl}_2$  at 298 K; <sup>b</sup> Recorded at 298 K in deaerated  $\text{CH}_2\text{Cl}_2$  solution ( $\lambda_{\text{exc}} = 420$  nm); <sup>c</sup>  $[\text{Ru}(\text{bpy})_3]\text{PF}_6$  in MeCN as the reference ( $\Phi_{\text{PL}} = 1.8\%$  in aerated MeCN at 298 K)[50]; <sup>d</sup>  $\lambda_{\text{exc}} = 378$  nm.

### *Dye-sensitized solar cells (DSSCs)*

Sandwich-type solar cells were assembled using **1**-sensitized nanocrystalline  $\text{TiO}_2$  as the working electrodes, platinized conducting glass as the counter electrode and iodide/triiodide in acetonitrile as electrolyte. The photovoltaic performances of solar cells based **1** and **N719**, as benchmark sensitizer, are summarized in Table 3. Figure 7 shows the current–voltage characteristics of the dyes under AM 1.5 simulated sunlight ( $100 \text{ mW cm}^{-2}$ ) and in the dark.

Table 3. Photovoltaic performance of **1**.

DYE	$J_{\text{sc}}^{\text{a}} / \text{mA cm}^{-2}$	$V_{\text{oc}}^{\text{a}} / \text{V}$	$\text{FF}^{\text{a}}$	$\eta^{\text{a}} / \%$
<b>1</b>	0.995	0.67	0.74	0.49
<b>N719</b>	8.84	0.81	0.61	4.4

<sup>a</sup>  $J_{\text{sc}}$  is the short-circuit current density at the  $V = 0$  intercept,  $V_{\text{oc}}$  is the open-circuit voltage at the  $J = 0$  intercept,  $\text{FF}$  is the device fill factor,  $\eta$  is the power conversion efficiency.

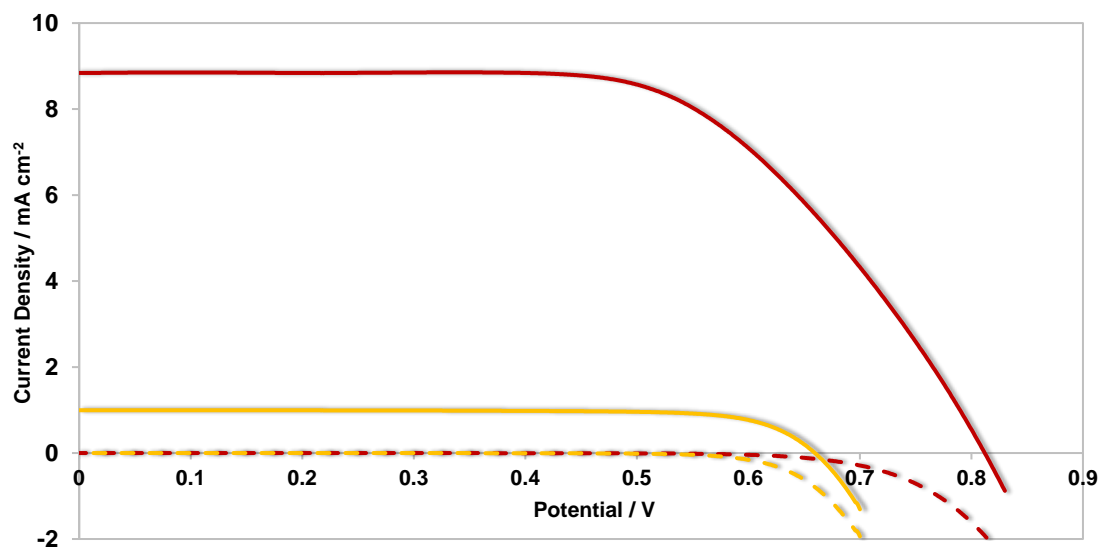


Figure 7. Current-voltage curves for DSSCs constructed using **1** (orange) and **N719** (red) in the dark (dashed line) and under simulated sunlight (solid line, AM1.5, 100 mW cm<sup>-2</sup>).

The photovoltaic efficiency ( $\eta = 0.49\%$ ) obtained with **1** is low, but comparable with results for iridium sensitizers reported elsewhere.[10,9,8,7,5] Both charge injection from the excited dye into TiO<sub>2</sub> and regeneration by the electrolyte are thermodynamically favourable. The fill factor for the N719 device (0.61) was slightly lower than typically obtained in optimized devices (0.70-0.75) and the shape of the current-voltage curve is consistent with high series resistance. Procedures used in optimized N719 devices, such as mixed solvents or additives such as chenodeoxycholic acid in the electrolyte or dye bath are likely to improve the performance of the N719 devices, however the conditions chosen were optimal for compound **1**. We therefore attribute the reason for the low efficiency for **1** compared to the benchmark Ru dye to be the weak absorption in the visible region, compared to ruthenium-based photosensitizers such as N719. The absorption spectrum of the TiO<sub>2</sub> electrode after immersion in the dye solution is provided in Figure S13 and the spectral response of the DSSC is given in Figure S14. The low incident photon-to current

conversion efficiency (IPCE < 2%) is consistent with the poor light-harvesting at  $\lambda > 500$  nm. While these dyes absorb broadly across the visible spectrum, the low  $\epsilon$  ( $\epsilon \sim 2\,000\text{ M}^{-1}\text{ cm}^{-1}$ ) compared to ruthenium dyes ( $\epsilon > 10\,000\text{ M}^{-1}\text{ cm}^{-1}$ ) is a limitation to their solar cell performance.

## Conclusions

In conclusion, a new panchromatically absorbing, NIR luminescent iridium(III) complexes bearing a tripodal tris(six-membered) chelate ligand has been obtained and comprehensively characterized, including by single crystal X-ray diffraction. The absorption spectrum tails off at 700 nm, much further than most neutral iridium complexes while the emission is significantly shifted into the NIR, with a maximum of 731 nm. DSSCs using **1** as the dye achieved only modest efficiency of 0.49%, comparable to other Ir(III) dyes. This was attributed to the modest absorption coefficient, which leads to weak light harvesting in the visible region and low short-circuit current.

## Experimental

### Dye sensitised solar cell fabrication

FTO glass substrates (TEC 15) were cleaned by ultrasonication in dilute soapy water, 0.1 M HCl in ethanol, and ethanol for 15 minutes each. A  $\text{TiCl}_4$  blocking layer was deposited by immersing the substrates into 20 mM  $\text{TiCl}_4$  solution and heating to 75 °C for 30 min, then washing with water and ethanol.  $\text{TiO}_2$  films were prepared by a doctor blading method in which a transparent  $\text{TiO}_2$  paste (DSL 18NR-T, Dyesol) was deposited by spreading with a glass rod. Masks to determine thickness and film size ( $0.20\text{ cm}^2$ ) were made using Scotch Magic Tape. The films were dried by heating to 80 °C on a hotplate for 5 minutes. In some cases, a  $\text{TiO}_2$  scattering layer (Ti Nanoxide R/SP, Solaronix) was applied. The films were sintered (450 °C, 30 min, 30 min ramp time) and

upon cooling, another  $\text{TiCl}_4$  treatment was applied. The films were placed into dye baths containing 0.3 mM of Complex **1** (the best results were obtained when DCM was used as a solvent), and left in the dark for 24 hours before testing. Control dye baths contained 0.3 mM N719 in a 1:1 ratio of t-butanol and acetonitrile.

The Pt catalyst was deposited on the FTO glass by coating with  $10 \mu\text{L cm}^{-2}$  of  $\text{H}_2\text{PtCl}_6$  solution (5 mM in isopropanol), followed by heating at  $400^\circ\text{C}$  for 15 minutes. Cells were constructed using the as-prepared films sandwiched with a Pt-coated FTO glass counter electrode (TEC 8), using Surlyn as a spacer. An iodine redox electrolyte composed of 0.6 M TBAI, 0.03 M  $\text{I}_2$ , 0.1 M guanidinium thiocyanate and 0.5 M t-butyl pyridine in MeCN was introduced into cells via a pre-drilled hole in the counter electrode, which were then sealed with another piece of Surlyn and a glass coverslip. The cells were masked with an aperture 1mm wider than the active area. The current–voltage characteristics of the DSSCs were recorded under AM 1.5 simulated sunlight ( $100 \text{ mW cm}^{-2}$ ) and in the dark. The best of a catch of four cells is reported, with results for each set agreeing within 10% for  $J_{\text{sc}}$  and 2% for  $V_{\text{oc}}$ .

## Acknowledgements

C.H. acknowledges the *Région Bretagne*, France for funding. EZ-C acknowledges the University of St Andrews and EPSRC (EP/M02105X/1) for financial support. We thank Umicore AG for the gift of materials. We thank the EPSRC UK National Mass Spectrometry Facility at Swansea University for analytical services. This research used computational resources of 1) the GENCI-CINES/IDRIS, 2) the CCIPL (*Centre de Calcul Intensif des Pays de Loire*), 3) a local Troy cluster. EAG and HVF thank the ERC for a Starting Grant (p-TYPE, 715354).

**Supporting information.** X-ray crystallographic structure of **1** in CIF format (CCDC: 1583853). NMR and MS spectra for **1**, Supplementary crystallographic data, supplementary electrochemical and photophysical data. Description of the DFT/TD-DFT protocol. Experimental details for the DSSC assembly and testing. Plots of the absorption spectra of **1**-sensitized TiO<sub>2</sub> and IPCE spectrum of the DSSC.

## References

1. Henwood, A.F., Zysman-Colman, E.: A Comprehensive Review of Luminescent Iridium Complexes Used in Light-Emitting Electrochemical Cells (LEECs). In: *Iridium(III) in Optoelectronic and Photonics Applications*. pp. 275-357. John Wiley & Sons, Ltd, (2017)
2. Longhi, E., De Cola, L.: Iridium(III) Complexes for OLED Application. In: *Iridium(III) in Optoelectronic and Photonics Applications*. pp. 205-274. John Wiley & Sons, Ltd, (2017)
3. Mayo, E.I., Kilsa, K., Tirrell, T., Djurovich, P.I., Tamayo, A., Thompson, M.E., Lewis, N.S., Gray, H.B.: Cyclometalated iridium(iii)-sensitized titanium dioxide solar cells. *Photochem. Photobiol. Sci* **5**(10), 871-873 (2006).
4. Yuan, Y.-J., Zhang, J.-Y., Yu, Z.-T., Feng, J.-Y., Luo, W.-J., Ye, J.-H., Zou, Z.-G.: Impact of Ligand Modification on Hydrogen Photogeneration and Light-Harvesting Applications Using Cyclometalated Iridium Complexes. *Inorg. Chem.* **51**, 4123-4133 (2012). doi:10.1021/ic202423y



5. Dragonetti, C., Valore, A., Colombo, A., Righetto, S., Trifiletti, V.: Simple novel cyclometallated iridium complexes for potential application in dye-sensitized solar cells. *Inorg. Chim. Acta* **388**(0), 163-167 (2012). doi:10.1016/j.ica.2012.03.028
6. Ning, Z., Zhang, Q., Wu, W., Tian, H.: Novel iridium complex with carboxyl pyridyl ligand for dye-sensitized solar cells: High fluorescence intensity, high electron injection efficiency? *J. Organomet. Chem.* **694**(17), 2705-2711 (2009). doi:10.1016/j.jorganchem.2009.02.016
7. Baranoff, E., Yum, J.-H., Graetzel, M., Nazeeruddin, M.K.: Cyclometallated iridium complexes for conversion of light into electricity and electricity into light. *J. Organomet. Chem.* **694**(17), 2661-2670 (2009). doi:10.1016/j.jorganchem.2009.02.033
8. Baranoff, E., Yum, J.-H., Jung, I., Vulcano, R., Grätzel, M., Nazeeruddin, M.K.: Cyclometallated Iridium Complexes as Sensitizers for Dye-Sensitized Solar Cells. *Chem. Asian J.* **5**(3), 496-499 (2010). doi:10.1002/asia.200900429
9. Sinopoli, A., Wood, C.J., Gibson, E.A., Elliott, P.I.P.: New cyclometalated iridium(III) dye chromophore complexes for n-type dye-sensitized solar cells. *Inorg. Chim. Acta* **457**, 81-89 (2017). doi:10.1016/j.ica.2016.12.003
10. Sinopoli, A., Wood, C.J., Gibson, E.A., Elliott, P.I.P.: Hybrid Cyclometalated Iridium Coumarin Complex as a Sensitizer of Both n- and p-Type DSSCs. *Eur. J. Inorg. Chem.* **2016**(18), 2887-2890 (2016). doi:10.1002/ejic.201600242
11. Wang, D., Wu, Y., Dong, H., Qin, Z., Zhao, D., Yu, Y., Zhou, G., Jiao, B., Wu, Z., Gao, M., Wang, G.: Iridium (III) complexes with 5,5-dimethyl-3-(pyridin-2-yl)cyclohex-2-enone ligands as sensitizer for dye-sensitized solar cells. *Org. Electron.* **14**(12), 3297-3305 (2013). doi:10.1016/j.orgel.2013.09.040
12. Shinpuku, Y., Inui, F., Nakai, M., Nakabayashi, Y.: Synthesis and characterization of novel cyclometalated iridium(III) complexes for nanocrystalline TiO<sub>2</sub>-based dye-sensitized solar cells. *J. Photochem. Photobiol., A* **222**(1), 203-209 (2011). doi:10.1016/j.jphotochem.2011.05.023
13. Gennari, M., Légalité, F., Zhang, L., Pellegrin, Y., Blart, E., Fortage, J., Brown, A.M., Deronzier, A., Collomb, M.-N., Boujtita, M., Jacquemin, D., Hammarström, L., Odobel, F.: Long-Lived Charge Separated State in NiO-Based p-Type Dye-Sensitized Solar Cells with Simple Cyclometalated Iridium Complexes. *The Journal of Physical Chemistry Letters* **5**(13), 2254-2258 (2014). doi:10.1021/jz5009714
14. Henwood, A.F., Hu, Y., Sajjad, M.T., Thalluri, G.K., Ghosh, S.S., Cordes, D.B., Slawin, A.M., Samuel, I.D., Robertson, N., Zysman-Colman, E.: Unprecedented Strong Panchromatic Absorption from Proton-Switchable Iridium(III) Azoimidazolate Complexes. *Chem. Eur. J.* **21**(52), 19128-19135 (2015). doi:10.1002/chem.201503546
15. Hasan, K., Zysman-Colman, E.: Panchromatic Cationic Iridium(III) Complexes. *Inorg. Chem. ASAP*, DOI: 10.1021/ic301998t (2012). doi:10.1021/ic301998t
16. Tamayo, A.B., Garon, S., Sajoto, T., Djurovich, P.I., Tsyba, I.M., Bau, R., Thompson, M.E.: Cationic Bis-cyclometalated Iridium(III) Diimine Complexes and Their Use in Efficient Blue, Green, and Red Electroluminescent Devices. *Inorg. Chem.* **44**(24), 8723-8732 (2005). doi:10.1021/ic050970t
17. Zhao, Q., Liu, S., Shi, M., Wang, C., Yu, M., Li, L., Li, F., Yi, T., Huang, C.: Series of New Cationic Iridium(III) Complexes with Tunable Emission Wavelength and Excited State Properties: Structures, Theoretical Calculations, and Photophysical and

- Electrochemical Properties. *Inorg. Chem.* **45**(16), 6152-6160 (2006).  
doi:doi:10.1021/ic052034j
18. Medina-Castillo, A.L., Fernandez-Sanchez, J.F., Klein, C., Nazeeruddin, M.K., Segura-Carretero, A., Fernandez-Gutierrez, A., Graetzel, M., Spichiger-Keller, U.E.: Engineering of efficient phosphorescent iridium cationic complex for developing oxygen-sensitive polymeric and nanostructured films. *Analyst* **132**(9), 929-936 (2007).
  19. Aubert, V., Ordonneau, L., Escadeillas, M., Williams, J.A.G., Boucekkine, A., Coulaud, E., Dragonetti, C., Righetto, S., Roberto, D., Ugo, R., Valore, A., Singh, A., Zyss, J., Ledoux-Rak, I., Le Bozec, H., Guerchais, V.r.: Linear and Nonlinear Optical Properties of Cationic Bipyridyl Iridium(III) Complexes: Tunable and Photoswitchable? *Inorg. Chem.* **50**(11), 5027-5038 (2011). doi:10.1021/ic2002892
  20. Kammer, S., Starke, I., Pietrucha, A., Kelling, A., Mickler, W., Schilde, U., Dosche, C., Kleinpeter, E., Holdt, H.-J.: 1,12-Diazaperylene and 2,11-dialkylated-1,12-diazaperylene iridium(III) complexes  $[\text{Ir}(\text{C}^{\wedge}\text{N})_2(\text{N}^{\wedge}\text{N})]\text{PF}_6$ : new supramolecular assemblies. *Dalton Trans.* **41**(34), 10219-10227 (2012).
  21. Hierlinger, C., Roisnel, T., Cordes, D.B., Slawin, A.M.Z., Jacquemin, D., Guerchais, V., Zysman-Colman, E.: An Unprecedented Family of Luminescent Iridium(III) Complexes Bearing a Six-Membered Chelated Tridentate  $\text{C}^{\wedge}\text{N}^{\wedge}\text{C}$  Ligand. *Inorg Chem* **56**(9), 5182-5188 (2017). doi:10.1021/acs.inorgchem.7b00328
  22. He, W.Y., Fontmorin, J.M., Hapiot, P., Soutrel, I., Floner, D., Fourcade, F., Amrane, A., Geneste, F.: A new bipyridyl cobalt complex for reductive dechlorination of pesticides. *Electrochim. Acta* **207**, 313-320 (2016). doi:10.1016/j.electacta.2016.04.170
  23. Koga, Y., Kamo, M., Yamada, Y., Matsumoto, T., Matsubara, K.: Synthesis, Structures, and Unique Luminescent Properties of Tridentate  $\text{C}^{\wedge}\text{C}^{\wedge}\text{N}$  Cyclometalated Complexes of Iridium. *Eur. J. Inorg. Chem.* **2011**(18), 2869-2878 (2011). doi:10.1002/ejic.201100055
  24. Obara, S., Itabashi, M., Okuda, F., Tamaki, S., Tanabe, Y., Ishii, Y., Nozaki, K., Haga, M.-a.: Highly Phosphorescent Iridium Complexes Containing Both Tridentate Bis(benzimidazolyl)-benzene or -pyridine and Bidentate Phenylpyridine: Synthesis, Photophysical Properties, and Theoretical Study of Ir-Bis(benzimidazolyl)benzene Complex. *Inorg. Chem.* **45**(22), 8907-8921 (2006). doi:doi:10.1021/ic060796o
  25. Brulatti, P., Gildea, R.J., Howard, J.A.K., Fattori, V., Cocchi, M., Williams, J.A.G.: Luminescent Iridium(III) Complexes with  $\text{N}^{\wedge}\text{C}^{\wedge}\text{N}$ -Coordinated Terdentate Ligands: Dual Tuning of the Emission Energy and Application to Organic Light-Emitting Devices. *Inorg. Chem.* **51**(6), 3813-3826 (2012). doi:10.1021/ic202756w
  26. Ashizawa, M., Yang, L., Kobayashi, K., Sato, H., Yamagishi, A., Okuda, F., Harada, T., Kuroda, R., Haga, M.A.: Syntheses and photophysical properties of optical-active blue-phosphorescent iridium complexes bearing asymmetric tridentate ligands. *Dalton Trans*(10), 1700-1702 (2009). doi:10.1039/b820821m
  27. Daniels, R.E., Culham, S., Hunter, M., Durrant, M.C., Probert, M.R., Clegg, W., Williams, J.A., Kozhevnikov, V.N.: When two are better than one: bright phosphorescence from non-stereogenic dinuclear iridium(III) complexes. *Dalton Trans* **45**(16), 6949-6962 (2016). doi:10.1039/c6dt00881j
  28. Yoshikawa, N., Sakamoto, J., Kanehisa, N., Kai, Y., Matsumura-Inoue, T., Takashima, H., Tsukahara, K.: (4,4'-Dimethyl-2,2'-bipyridine)chloro-(2,2':6',2''-terpyridine)-iridium(III)

- hexafluorophosphate. *Acta Cryst. E* **59**(10), m830-m832 (2003).  
doi:10.1107/s1600536803019081
29. Hanss, D., Freys, J.C., Bernardinelli, G., Wenger, O.S.: Cyclometalated Iridium(III) Complexes as Photosensitizers for Long-Range Electron Transfer: Occurrence of a Coulomb Barrier. *Eur. J. Inorg. Chem.* **2009**(32), 4850-4859 (2009).  
doi:10.1002/ejic.200900673
  30. Henwood, A.F., Pal, A.K., Cordes, D.B., Slawin, A.M.Z., Rees, T.W., Momblona, C., Babaei, A., Pertegas, A., Orti, E., Bolink, H.J., Baranoff, E., Zysman-Colman, E.: Blue-emitting cationic iridium(III) complexes featuring pyridylpyrimidine ligands and their use in sky-blue electroluminescent devices. *J. Mater. Chem. C* **5**(37), 9638-9650 (2017).  
doi:10.1039/C7TC03110F
  31. Costa, R.D., Orti, E., Bolink, H.J., Graber, S., Schaffner, S., Neuburger, M., Housecroft, C.E., Constable, E.C.: Archetype Cationic Iridium Complexes and Their Use in Solid-State Light-Emitting Electrochemical Cells. *Adv. Funct. Mater.* **19**(21), 3456-3463 (2009). doi:10.1002/adfm.200900911
  32. Ladouceur, S., Fortin, D., Zysman-Colman, E.: The role of substitution on the photophysical properties of 5,5'-diaryl-2,2'-bipyridine (bpy\*) in [Ir(ppy)<sub>2</sub>(bpy\*)]PF<sub>6</sub> complexes: A combined experimental and theoretical study. *Inorg. Chem.* **49**(12), 5625-5641 (2010).  
doi:10.1021/ic100521t/
  33. Liu, S.-J., Zhao, Q., Fan, Q.-L., Huang, W.: A Series of Red-Light-Emitting Ionic Iridium Complexes: Structures, Excited State Properties, and Application in Electroluminescent Devices. *Eur. J. Inorg. Chem.* **2008**(13), 2177-2185 (2008). doi:10.1002/ejic.200701184
  34. Cardona, C.M., Li, W., Kaifer, A.E., Stockdale, D., Bazan, G.C.: Electrochemical Considerations for Determining Absolute Frontier Orbital Energy Levels of Conjugated Polymers for Solar Cell Applications. *Adv. Mater.* **23**(20), 2367-2371 (2011).  
doi:10.1002/adma.201004554
  35. Chirdon, D.N., McCusker, C.E., Castellano, F.N., Bernhard, S.: Tracking of Tuning Effects in Bis-Cyclometalated Iridium Complexes: A Combined Time Resolved Infrared Spectroscopy, Electrochemical, and Computational Study. *Inorg. Chem.* **52**(15), 8795-8804 (2013). doi:10.1021/ic401009q
  36. Pavlishchuk, V.V., Addison, A.W.: Conversion constants for redox potentials measured versus different reference electrodes in acetonitrile solutions at 25°C. *Inorg. Chim. Acta* **298**(1), 97-102 (2000). doi:10.1016/s0020-1693(99)00407-7
  37. Connelly, N.G., Geiger, W.E.: Chemical Redox Agents for Organometallic Chemistry. *Chem. Rev.* **96**, 877-910 (1996).
  38. Zhao, Q., Yu, M., Shi, L., Liu, S., Li, C., Shi, M., Zhou, Z., Huang, C., Li, F.: Cationic Iridium(III) Complexes with Tunable Emission Color as Phosphorescent Dyes for Live Cell Imaging. *Organometallics* **29**(5), 1085-1091 (2010). doi:10.1021/om900691r
  39. Ertl, C.D., Momblona, C., Pertegás, A., Junquera-Hernández, J.M., La-Placa, M.-G., Prescimone, A., Ortí, E., Housecroft, C.E., Constable, E.C., Bolink, H.J.: Highly Stable Red-Light-Emitting Electrochemical Cells. *J. Am. Chem. Soc.* **139**(8), 3237-3248 (2017).  
doi:10.1021/jacs.6b13311
  40. Pal, A.K., Cordes, D.B., Slawin, A.M.Z., Momblona, C., Pertegas, A., Orti, E., Bolink, H.J., Zysman-Colman, E.: Simple design to achieve red-to-near-infrared emissive cationic Ir(III) emitters and their use in light emitting electrochemical cells. *RSC Advances* **7**(51), 31833-31837 (2017). doi:10.1039/C7RA06347D

41. Kesarkar, S., Mróz, W., Penconi, M., Pasini, M., Destri, S., Cazzaniga, M., Ceresoli, D., Mussini, P.R., Baldoli, C., Giovannella, U., Bossi, A.: Near-IR Emitting Iridium(III) Complexes with Heteroaromatic  $\beta$ -Diketonate Ancillary Ligands for Efficient Solution-Processed OLEDs: Structure–Property Correlations. *Angew. Chem. Int. Ed.* **55**(8), 2714–2718 (2016). doi:10.1002/anie.201509798
42. Xin, L., Xue, J., Lei, G., Qiao, J.: Efficient near-infrared-emitting cationic iridium complexes based on highly conjugated cyclometalated benzo[g]phthalazine derivatives. *RSC Adv.* **5**(53), 42354–42361 (2015). doi:10.1039/c5ra04511h
43. Zhang, G., Zhang, H., Gao, Y., Tao, R., Xin, L., Yi, J., Li, F., Liu, W., Qiao, J.: Near-Infrared-Emitting Iridium(III) Complexes as Phosphorescent Dyes for Live Cell Imaging. *Organometallics* **33**(1), 61–68 (2013). doi:10.1021/om400676h
44. Tao, R., Qiao, J., Zhang, G., Duan, L., Wang, L., Qiu, Y.: Efficient Near-Infrared-Emitting Cationic Iridium Complexes as Dopants for OLEDs with Small Efficiency Roll-off. *J. Phys. Chem. C* **116**(21), 11658–11664 (2012). doi:10.1021/jp301740c
45. Hasan, K., Bansal, A.K., Samuel, I.D.W., Roldán-Carmona, C., Bolink, H.J., Zysman-Colman, E.: Tuning the Emission of Cationic Iridium (III) Complexes Towards the Red Through Methoxy Substitution of the Cyclometalating Ligand. *Scientific Reports* **5**, 12325 (2015). doi:10.1038/srep12325
46. Wang, L., Yin, H., Cui, P., Hetu, M., Wang, C., Monro, S., Schaller, R.D., Cameron, C.G., Liu, B., Kilina, S., McFarland, S.A., Sun, W.: Near-infrared-emitting heteroleptic cationic iridium complexes derived from 2,3-diphenylbenzo[g]quinoxaline as in vitro theranostic photodynamic therapy agents. *Dalton Trans.* **46**(25), 8091–8103 (2017). doi:10.1039/C7DT00913E
47. Xin, L., Xue, J., Lei, G., Qiao, J.: Efficient near-infrared-emitting cationic iridium complexes based on highly conjugated cyclometalated benzo[g]phthalazine derivatives. *RSC Advances* **5**(53), 42354–42361 (2015). doi:10.1039/C5RA04511H
48. Cao, X., Miao, J., Zhu, M., Zhong, C., Yang, C., Wu, H., Qin, J., Cao, Y.: Near-Infrared Polymer Light-Emitting Diodes with High Efficiency and Low Efficiency Roll-off by Using Solution-Processed Iridium(III) Phosphors. *Chem. Mater.* **27**(1), 96–104 (2015). doi:10.1021/cm503361j
49. Tao, R., Qiao, J., Zhang, G., Duan, L., Chen, C., Wang, L., Qiu, Y.: High-efficiency near-infrared organic light-emitting devices based on an iridium complex with negligible efficiency roll-off. *J. Mater. Chem. C* **1**(39), 6446–6454 (2013). doi:10.1039/C3TC30866A
50. Suzuki, K., Kobayashi, A., Kaneko, S., Takehira, K., Yoshihara, T., Ishida, H., Shiina, Y., Oishi, S., Tobita, S.: Reevaluation of absolute luminescence quantum yields of standard solutions using a spectrometer with an integrating sphere and a back-thinned CCD detector. *Phys Chem Chem Phys* **11**(42), 9850–9860 (2009). doi:10.1039/b912178a

